Dear Author,

Please, note that changes made to the HTML content will be added to the article before publication, but are not reflected in this PDF.

Note also that this file should not be used for submitting corrections.

Electrochimica Acta xxx (2015) xxx–xxx

Contents lists available at ScienceDirect

Electrochimica Acta

journal homepage: www.elsevier.com/locate/electacta

Electrochemical detection of cupric ions with boron-doped diamond electrode for marine corrosion monitoring

M. Nie[a,*,1], S. Neodo[a], J.A. Wharton[a,1], A. Cranny[b], N.R. Harris[b], R.J.K. Wood[a], K.R. Stokes[a,c]

[a] National Centre for Advanced Tribology at Southampton (nCATS), Faculty of Engineering and the Environment, University of Southampton, Southampton, SO17 1BJ, UK
[b] Electronics and Computer Science, Faculty of Physical Sciences and Engineering, University of Southampton, Southampton, SO17 1BJ, UK
[c] Platform Systems Division, Dstl, Porton Down, Salisbury, SP4 0JQ, UK

ARTICLE INFO

Article history:
Received 19 August 2015
Received in revised form 28 December 2015
Accepted 28 December 2015
Available online xxx

Keywords:
Electrochemical sensing
Boron-doped diamond
Marine corrosion monitoring
Differential pulse voltammetry

ABSTRACT

Corrosion induced structural failures continue to be a costly problem in many industrial situations, and the development of robust corrosion sensing systems for structural health integrity monitoring is still a demanding challenge. The applicability of corrosion monitoring of copper alloys using a boron-doped diamond electrode (BDD) has been performed based on determination of copper ions within localised corrosion microenvironments. The electrochemical behaviour of copper ions on the BDD electrode surface were first reported in details in 0.60 M NaCl aqueous solution, and the results revealed that the electrochemical processes of copper ions on the BDD electrode proceed as two successive single electron transfer steps producing two well-separated pairs of peaks in cyclic voltammograms in the chloride ion containing electrolyte solutions. Compared with perchlorate and sulphate ions, chloride ions were observed with a significant stabilization effect on copper ions via the formation of $CuCl_2^-$ complex, thus having two well-separated pairs of peaks in the obtained cyclic voltammograms on the BDD electrode in the chloride ion electrolyte solution. The apparent rate constant for the redox couple of Cu^{2+}/Cu^+ in chloride ion electrolyte was determined as 0.94×10^{-6} cm s^{-1} by using quasi-steady polarisation technique, thus indicating a quasi-reversible electron transfer process of Cu^{2+}/Cu^+ redox couple. Moreover, differential pulse voltammetric results exhibited the BDD electrode is promising for corrosion monitoring of copper alloys with an excellent relationship between peak current and concentration of copper ions without significant interference from the commonly presented metal ions within the simulated marine corrosion environments.

1. Introduction

Electrochemical detection technology has recently attracted significant attention among the development of fully-integrated sensing systems, due to its inherent miniaturization, low-power requirements, low limits of detection, compatibility with advanced micromachining systems, low instrumentation cost, and relative simplicity regarding to the procedure protocols [1–3]. Research into new and effective electrode materials has been chiefly driven in order to improve existing electrochemical sensing systems and to design new ones. Noble metals, such as platinum and gold, with excellent chemical inertness, are often considered as the mainstays in the electroanalytical field. However, the detection of various analytes in aqueous media is often not feasible at high overpotentials, since these often result in either oxygen or hydrogen evolution on these metal electrodes in aqueous media [4]. In the past, due to the high overpotential towards hydrogen evolution, mercury electrodes were extensively exploited for trace metal analysis, however, its toxicity has promoted alternative research efforts to find replacements using less or non-harmful materials [5].

Boron-doped diamond (BDD) is increasingly of interest since its outstanding chemical and physical properties are unparalleled in comparison with other electrode materials [3–7]. The nil toxicity, the high overpotentials for oxygen and hydrogen evolutions [8], the high chemical and physical stability in addition to the low capacitive current in aqueous solutions [9], make BDD an attractive electrode material widely used in electroanalysis. One of the most extensively investigated BDD characteristics is the surface

* Corresponding author. Tel.: +44 23 8059 3761; fax: +44 23 8059 3016.
E-mail addresses: mynie105@hotmail.com, m.nie@soton.ac.uk (M. Nie), sn1d09@soton.ac.uk (S. Neodo), awc@ecs.soton.ac.uk (A. Cranny), nrh@ecs.soton.ac.uk (N.R. Harris), r.wood@soton.ac.uk (R.J.K. Wood), krstokes@mail.dstl.gov.uk (K.R. Stokes).
[1] ISE member.

http://dx.doi.org/10.1016/j.electacta.2015.12.194
0013-4686/

property and its influence on the electron transfer process. It has been widely shown that the electrochemical properties of the diamond electrode depend not only on the surface state, such as oxygen-, hydrogen- or fluorine- termination, but also on the way the surface modification is performed [10–17]. The advantages of BDD over conventional noble metals, carbon paste and glassy carbon electrodes in quantification of metal ions have been reported for the determination of trace metal ions for a broad range of examples: such as mercury in flue gas power plant sample [18], manganese in seawater [19] and marine sediment [20], arsenic in well water [21], and lead in river sediment [22].

Corrosion induced structural failure continues to be a costly problem in many industrial situations, especially for marine structures and platforms. The structural health integrity of marine structures can critically be affected by corrosion, in particular by localized corrosion, such as pitting and crevice corrosion. However, localized corrosion is extremely problematic to effectively detect due to limited access to affected areas, and the lack of robust corrosion sensing systems [23]. For example, non-destructive evaluation (NDE) methods, such as acoustic emission (AE), ultrasonic, and infrared thermography, have been improved significantly in recent years for inspection of pipelines and other large complex structures. However, these techniques are time consuming, and the limitations (e.g. service environment noise, temperature and access) associated with these methods cannot guarantee the inspection outcomes [24]. Electrochemical techniques have also been widely used to monitor corrosion rate of the structures or service environments corrosivity, but the reliability of these techniques is still limited for *in situ* corrosion monitoring, as summarized in Table 1. Chemical imaging methods have recently been proven more accurate in monitoring localized corrosion process by measuring local concentration of oxygen or ionic species (e.g. H^+ and/or metallic ions) at sites of interest using ion-selective microelectrodes (ISME) or pH sensors [25–29]. However, the nature of these corrosive environments, such as marine (both coastal and oceanic), and the area of application are such that robust sensors are required with the minimum of maintenance and capable of sustained operation over long timescales. Compared with current ISMEs, BDD electrode would be a better option for such applications due to its mechanical robust and stable surface properties, great resistance to surface fouling, and excellent electroanalysis performance.

Copper-based alloys are extensively used in marine structures, and are liable to localized corrosion in marine environments. For the commonly used copper alloys in marine environment (cupronickels, aluminium and nickel-aluminium bronzes), copper ions are main species initially produced by the corrosion process, while other metal ions, such as ferric, nickel and aluminium ions, are sometimes also produced as by-products [30–32]. Wharton et al. proposed that levels of metal ions produced within corrosion solution microenvironments could be used for determination of corrosion initiation locations and life-prediction of metal structures [30,32]. Corrosion sensing systems for copper-based marine structural health monitoring are being developed based on electrochemical detection of metal ions produced by localized corrosion in our laboratory [33,34].

The electrochemical behaviour of copper on BDD electrodes is a subject of much attention due to its direct involvement in fundamental chemistry, in biological systems and in the industrial field. For example, Nakabayashi et al. [35] investigated the electrochemical response of the BDD and platinum electrodes to copper ions in 0.1 M sodium sulphate solution using cyclic voltammetry. They found that an intense reduction peak was observed on both BDD and platinum electrodes, but only a very small broad anodic peak was obtained with the BDD electrode compared to a strong sharp anodic stripping peak with the platinum electrode. This feature of a low anodic to cathodic charge ratio for the BDD electrodes in neutral sulphate solutions was attributed to the formation of the insulating oxide layer on the reduced copper clusters and the electrostatic repulsion between the BDD surface and the copper clusters, which force the reduced copper particles to peel off from the BDD surface and to diffuse away into the bulk solution [14,36]. Zak et al. [37] observed different cyclic voltammetric behaviour to copper ions on BDD electrodes in different electrolyte solutions of sulphuric, phosphoric and nitric acids using electrochemical atomic force microscopy. They reported that copper metal grains were formed and uniformly distributed over the diamond crystal facets during the cathodic process in the acidic solutions, then completely removed from the BDD surface with intensive anodic stripping peaks. They suggested that the thickness of the deposited metal layer on the BDD surface as well as the stripping signal in the anodic process may be influenced by the ability of the supporting electrolyte to form copper complexes. Tamilani et al. [38] also investigated the electrochemical reduction of copper ions on BDD films to explore the feasibility of electrochemical removal of copper from chemical-mechanical planarization generated wastewater. Based on their preliminary CV results, they proposed that in a 0.05 M potassium sulphate solution, copper ions were electrochemically deposited on the BDD surface in the form of copper clusters via either two successive one-electron transfer processes involving a combination of Cu^{2+}/Cu^+ and Cu^+/Cu^0 in pH 4 solution or three one-electron transfer processes with an additional Cu_2O/Cu^0 process in pH 6 solution. BDD electrodes have also been successfully employed for the determination of trace copper metal ions via anodic stripping voltammetry using nitric acid or acetate buffer solutions as the supporting electrolytes [5,39–41]. Nevertheless, these methods for determination of copper ions with BDD electrode critically depend on the use of specific supporting electrolyte and its concentration, and are not suitable for on-site detection of copper ions produced within the localized marine corrosion microenvironments.

This paper studies the feasibility of using BDD electrodes for corrosion monitoring of copper alloys. To our knowledge, the electrochemical behaviour of copper ions in chloride background electrolyte has not been fully understood on boron-doped

Table 1
Most commonly used electrochemical techniques for metallic structure corrosion monitoring [24].

Electrochemical techniques	Advantages	Limitations
Polarization resistance methods (PR)	Simple, rapid (typically within a few minutes), nearly non-destructive, good sensitivity to low corrosion rates	Only valid for general corrosion; Affected by solution resistance, scan rate and the presence of redox species
Electrochemical noise methods (EN)	Similar to PR methods; ability to indicate the type of corrosion	Data processing and interpretation complicated; Limited reliability.
Zero resistance ammetry (ZRA) and galvanic sensors	Better than PR or EN for fast localized corrosion processes in low resistance electrolyte	Accuracy influenced by time frame of corrosion, electrolyte nature and crevice geometry.
Coupled multielectrode array sensor systems (CMAS)	Ability to study localized corrosion and to quantify pitting and crevice corrosion.	High cost; Big data; Often underestimation of actual corrosion rate.

Please cite this article in press as: M. Nie, et al., Electrochemical detection of cupric ions with boron-doped diamond electrode for marine corrosion monitoring, Electrochim. Acta (2015), http://dx.doi.org/10.1016/j.electacta.2015.12.194

diamond electrodes, especially in high concentration chloride ions. Hence the electrochemical behaviour of copper ions on the BDD electrode was investigated in 0.60 M NaCl (equal to average salinity of seawater) as well as in a simulated corrosion microenvironments produced by copper alloy marine structures. The effect of electrolyte anions on the electrochemical behaviour of copper ions on the BDD were initially investigated in 0.60 M sodium perchlorate, 0.20 M sodium sulphate and 0.60 M sodium chloride solutions with cyclic voltammetry (CV) and quasi-steady polarisation techniques. Further experiments showed that copper ions can be detected with the BDD electrode using differential pulse voltammetry (DPV) technique in the concentration range of 1.0×10^{-5} M to 1.0×10^{-1} M without significant interference from Fe^{3+}, Ni^{2+} and Al^{3+} ions under the simulated marine corrosion conditions, suggesting that the BDD electrode is a promising material for corrosion monitoring of copper-based marine structures.

2. Experimental

2.1. Chemicals

All the solutions were prepared with deionised water (>18.2 MΩ cm), with chemicals of analytical grade purity as received from Sigma-Aldrich (Poole, UK). The $CuCl_2$ reagent was used for the study of electrochemical properties of copper ion in supporting electrolyte solutions containing chloride ions, while $CuSO_4$ was employed for the investigations in chloride-free

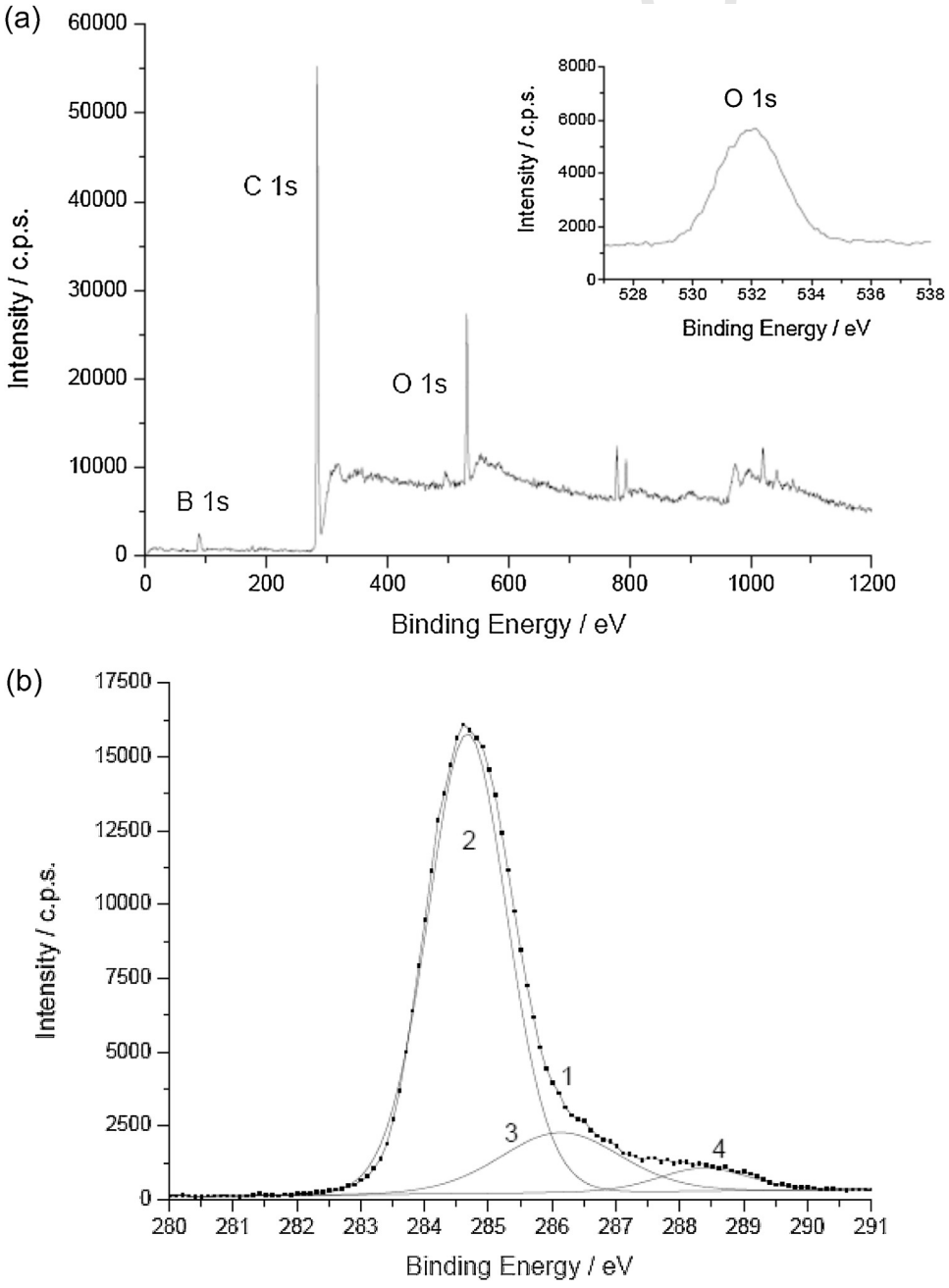

Fig. 1. XPS survey (a) and high resolution C1S (b) spectra of BDD electrode at an incident X-ray angle of 75°. Peaks 2, 3, 4 in (b) represent the fitted signals for the recorded peak 1 (dot-line).

Please cite this article in press as: M. Nie, et al., Electrochemical detection of cupric ions with boron-doped diamond electrode for marine corrosion monitoring, Electrochim. Acta (2015), http://dx.doi.org/10.1016/j.electacta.2015.12.194

supporting electrolyte solution. $NiCl_2$, $AlCl_3$ and $FeCl_3$ were also used for interference studies. Supporting electrolyte solutions were prepared using sodium chloride, sodium sulphate and sodium perchlorate. Copper ion testing solutions with concentrations down to 1.0×10^{-6} M was prepared by diluting freshly made stock solutions of 1.0×10^{-1} M with the supporting electrolyte.

2.2. BDD electrode

A BDD electrode disk with a diameter of 7.0 ± 0.2 mm and a thickness of 0.5 ± 0.1 mm was supplied by Diamond Detectors Ltd (Poole, UK). The active part of the BDD with nominal diameter of 3.0 ± 0.2 mm was surrounded by non-conductive intrinsic diamond matrix. The electrode was doped with a doping level of 10^{20} boron atoms cm^{-3} (or 2000 ppm of boron in precursor gas), and the surface was terminated with oxygen with surface roughness of ca. 5 nm estimated by atomic force microscopy (AFM). The BDD electrode was mounted in a polypropylene tube with a 7 mm internal diameter, an electrical connection was made on the rear surface and the electrode assembly was sealed using Araldite epoxy resin. The chemical composition of the BBD electrode surface was also characterized using a Kratos AXIS Ultra-DLD X-ray photoelectron spectrometer (XPS) with a monochromatic dual Al-Mg X-ray source.

2.3. Electrochemical measurements

Cyclic voltammetry, differential pulse voltammetry, quasi-steady polarization curves and chronocoulometry tests were performed at room temperature (ca. 20 °C) using a Gamry Reference 600 potentiostat (Gamry Instruments, USA) and a three-electrode, single-compartment glass cell. The BDD electrode was used as the working electrode, and a large area graphite rod and a standard silver/silver chloride (Ag/AgCl) electrode were served as the counter and the reference electrodes, respectively. All potentials reported with respect to the Ag/AgCl reference electrode. Unless otherwise stated, all the solutions used were not degassed as the ability to degas sample solutions rarely present itself under *in situ* corrosion monitoring conditions.

Prior to electrochemical measurements, the BDD electrode was cleaned in a fresh 0.50 M sulphuric acid solution by cycling in a potential range of –0.60 V to +1.25 V until a reproducible electrode response was achieved, and then rinsed with deionised water.

CVs were carried out at 10 mV s^{-1} with a step size of 1 mV as the default scanning condition, but also at 25, 50, 100, 200 and 300 mV s^{-1} in order to study the effect of the scan rate on the electrochemical response. A number of CV scans were performed for each investigation until reproducible results were observed and it is the data from the last cyclic scan that are reported here.

DPVs were carried out at 10 mV s^{-1} in the cathodic scan with a step potential of 2 mV, potential pulse size of 25 mV, interval time of 0.2 s and a pulse time of 0.1 s.

Chronocoulometric measurements were performed with 10 mM potassium ferricyanide, $K_3[Fe(CN)_6]$, in a 0.6 M sodium chloride solution by initially holding at +0.70 V for 10 s, for which no significant electrolysis took place, then stepping to –0.50 V, a negative potential sufficient to promote the reduction of ferricyanide to ferrocyanide. The charge sampling period for the measurements was 0.01 s.

Quasi-steady polarization curves were carried out under low-field approximation at a scan rate of 0.20 mV s^{-1} and a step potential size of 0.15 mV. Measurements were carried out in a potential interval of ±10 mV with respect to the open circuit potential (OCP), performing the scan from anodic to cathodic values.

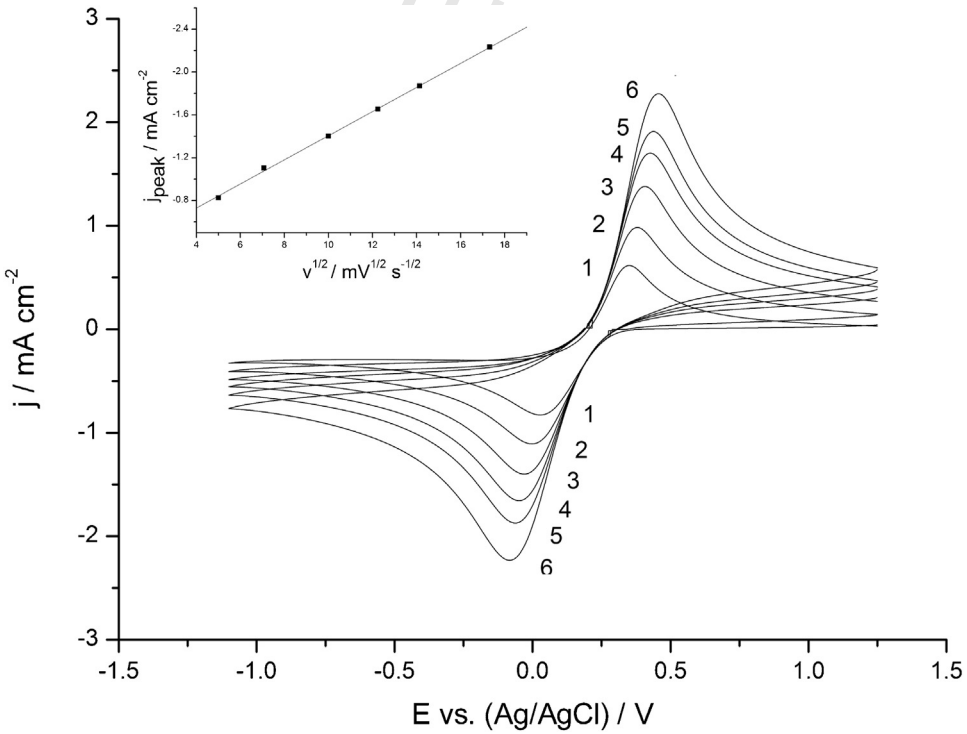

Fig. 2. Cyclic voltammograms of 10 mM $K_3[Fe(CN)_6]$ in 0.60 M NaCl solution, recorded at scan rates of (1) 10, (2) 25, (3) 50, (4) 100, (5) 200 and (6) 300 mV s^{-1}. Inset shows the trend of the reduction peak current density *vs.* the square root of the scan rate.

Please cite this article in press as: M. Nie, et al., Electrochemical detection of cupric ions with boron-doped diamond electrode for marine corrosion monitoring, Electrochim. Acta (2015), http://dx.doi.org/10.1016/j.electacta.2015.12.194

3. Results and discussion

3.1. Surface chemistry characterization of boron-doped diamond electrode

X-ray photoelectron spectroscopy (XPS) is a unique technique for understanding of surface chemistry by providing information of the average chemical composition of the topmost few nm of the surface. XPS measurements were carried out to assess the chemical functional groups present at the BDD electrode surface. As shown in Fig. 1a, the characteristic signal bands for the elements of carbon, oxygen and boron were observed in the XPS survey spectrum. The band centred at binding energy of 283.9 eV was attributed to C1s signal, while the bands at 530.9 eV and 189.9 eV were associated with O1s and B1s responses, respectively. The relative element abundance at the surface was also evaluated as 89.2% for carbon, 10.3% for oxygen, and 0.5% for boron, respectively.

Chemical-state analysis can reveal the local bonding environment of an element, such as its formal oxidation state, the identity of its nearest-neighbour atom and its bonding hybridization to that nearest-neighbour atom. Chemical-state analysis of the element carbon at the BBD electrode surface was also performed by fitting high energy resolution XPS spectrum. Fig. 1b shows that the fitting of C1s signal (dot-lined curve 1) produced three peaks, centred at 284.7 eV (peak 2), 286.1 eV (peak 3) and 288.4 eV (peak 4), respectively. According to the literature [42,43], the peaks can be assigned to the bulk diamond sp^3 carbon (C–C, peak 2), the alcohol/ether group carbon (C—OH/C—O—C, peak 3), and the carbonyl/carboxyl group carbon (C=O, peak 4). The relative carbon abundances for C—C, C—O, and C=O groups were determined as 79.7%, 15.7% and 4.5%, respectively. This revealed that around 20% of the total carbon content presented in the oxygen-containing functional groups at the BDD surface. These results are in good agreement with previous XPS studies on the oxygen-terminated BBD electrode [43], demonstrating that the surface of the BDD electrodes used in this study is oxygen-terminated. In addition, no obvious sp^2 graphitic carbon peak was detected from the chemical-state analysis of C1s spectrum, indicating that the commonly existed impurity graphite carbon is absent in the used BBD electrode surface. Therefore, the BDD electrodes used are oxygen-terminated at the surface with undetectable graphite impurity.

3.2. Electrochemical response of oxygen-terminated BDD for ferricyanide ion

The CV performance of the oxygen-terminated BDD (O-BDD) electrode was evaluated with the $[Fe(CN)_6]^{3-}/[Fe(CN)_6]^{4-}$ redox couple. Fig. 2 shows the CVs measured on the O-BDD electrode in 10 mM $K_3[Fe(CN)_6]$ in 0.60 M NaCl solution at different scan rates. As seen in the CVs, both reduction and oxidation peaks shift negatively and positively respectively, as the scan rate was increased. This electrochemical behaviour observed with the O-BDD electrode can be related to a quasi-reversible process, as previously reported [11,13]. An excellent linear relationship was also observed between the reduction peak current and the square root of scan rate, which indicates that the electrochemical behaviour of the studied redox couple on the O-BDD electrode is controlled by diffusion processes. These results demonstrated that the BDD electrode exhibited metal-like electrochemical performance [9].

In order to determine the real electroactive surface area of the used BDD electrode, single potential step chronocoulometry measurements were performed in 10 mM $K_3[Fe(CN)_6]$ in a 0.60 M NaCl solution. The potential applied was –0.5 V, sufficiently negative to promote the reduction of ferricyanide to ferrocyanide. The real electroactive electrode surface area can be calculated from the slope of the plot of the charge against the square root of the time according to the Anson equation [44]:

$$Q_d = \frac{2nFAC_o D_o^{1/2}}{\pi^{1/2}} t^{1/2} \quad (1)$$

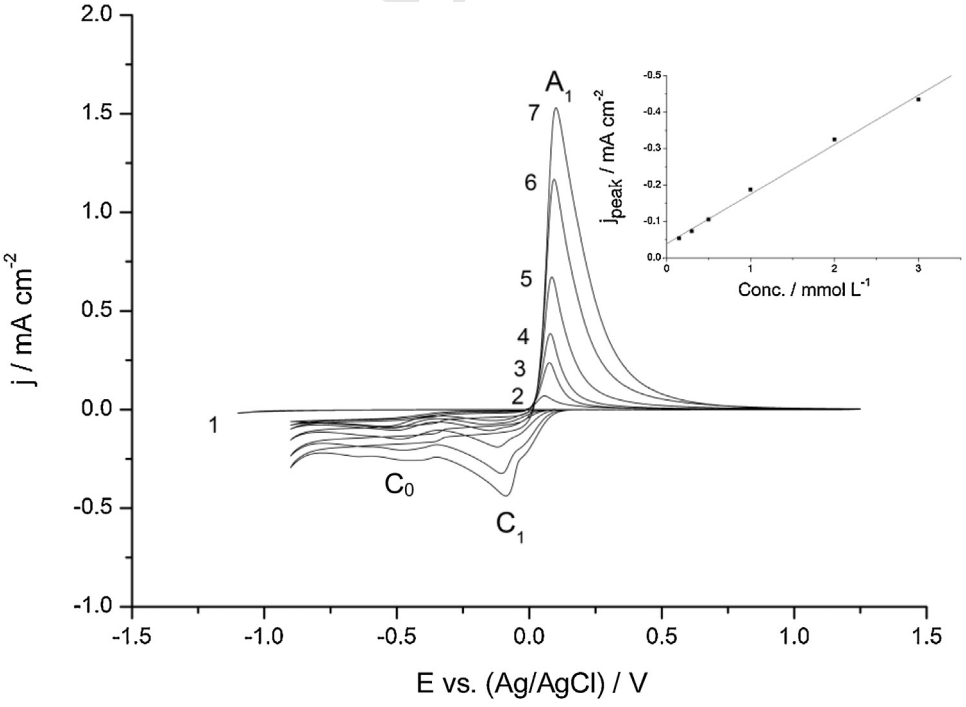

Fig. 3. Cyclic voltammograms of (1) 0, (2) 0.15, (3) 0.30, (4) 0.50, (5) 1.00, (6) 2.00 and (7) 3.00 mM $CuSO_4$ in 0.60 M $NaClO_4$ recorded at 10 mV s^{-1}. Inset shows the trend of the reduction peak (C_1) current density *vs.* copper ions concentration.

Please cite this article in press as: M. Nie, et al., Electrochemical detection of cupric ions with boron-doped diamond electrode for marine corrosion monitoring, Electrochim. Acta (2015), http://dx.doi.org/10.1016/j.electacta.2015.12.194

Thus, with a diffusion coefficient of 8.9×10^{-6} cm^2 s^{-1} for $K_3[Fe(CN)_6]$ [45], the real electroactive surface area of the BDD electrode used was calculated as 0.184 cm^2, which is about 2.5 times greater than the geometric electrode surface area. The difference between the estimated real surface area and the geometric surface area possibly results from the surface roughness of the BDD electrode introduced by mechanical polishing, the distorted atomic arrangements in surface layer, and surface defects [46].

3.3. Electrochemical behaviour of copper ions on O-BDD electrode

In order to better understand the influence of background electrolyte anions on the electrochemical behaviour of copper ions on the oxygen-terminated BDD electrode, CVs were performed in 0.60 M $NaClO_4$, 0.20 M Na_2SO_4 and 0.60 M NaCl solutions. All the electrolyte solutions with the aforementioned concentrations were prepared to maintain the same ionic strength at 0.60 M. Fig. 3 shows the CVs for $CuSO_4$ over the concentration range of zero to 3.0 mM in a 0.60 M $NaClO_4$ background electrolyte performed at 10 mV s^{-1}. It is apparent that the peaks A_1 and C_1 are attributed to oxidation and reduction of copper ions, respectively, as peak current densities for both peaks increased linearly with the increase of copper ions concentration (the inset in Fig. 3). In addition, the equilibrium potential for both peaks was observed to shift progressively from +0.005 V at the lowest copper ions concertation of 0.15 mM towards more positive values as the copper ions concentration increased; at 3.00 mM the equilibrium potential was determined to be +0.026 V. A slope of 27 mV dec^{-1} was determined from the plot of the estimated equilibrium potential against the copper ion concentration (not shown here), which is in good agreement with the theoretical value (29 mV dec^{-1} = 2.303 RT/2F) for a two-electron transfer process:

$$Cu^{2+} + 2e^- \leftrightarrow Cu^0_{ads} \quad (2)$$

Curve 1 in Fig. 3 shows negligible anodic and cathodic currents were produced in the potential range of -1.10 V to +1.25 V on the BBD electrodes in a solution containing 0.6 M $NaClO_4$ only, as expected on the BDD electrodes as a result of the high overpotentials for oxygen and hydrogen evolution reactions [8]. Although the dissolved oxygen was present in the solution at ca. 0.2 mM, no electrochemical response was detected for oxygen reduction reaction (ORR) in the blank solution on the BDD electrode. The same phenomenon of a low background current and no detectable ORR response was also observed in an aerated solution containing 0.60 M NaCl only on the BDD electrodes over the same potential range. This may be due to the higher overpotential for ORR on the BDD surface, the negligible non-diamond sp^2 carbon content within the used oxygen-terminated BDD electrode surface, and the low sensitivity of the used cyclic voltammetric technique at the low scan rate [8,47–51].

However, broad peak C_0 observed at around –0.50 V in curves 2-7 of Fig. 3 was confirmed with further experiments to be attributed to the reduction of dissolved oxygen in 0.60 M $NaClO_4$ solution, since this peak completely disappeared in the oxygen-free solution degassed by N_2, as seen in Fig. 4 (dotted line). The oxygen reduction signals observed in the naturally aerated solutions containing copper ions could be due to the electrochemically deposited metallic copper on the BDD electrode surface which effectively enhanced the catalytic activity to oxygen reduction [52–54]. Moreover, it is evident in Fig. 4 that the shoulder peak at around 0.0 V occurring at potentials slightly more positive to the main peak C_1, which could be related to a transient Cu(I) species, also disappeared when the solution was purged with nitrogen gas [35,38,55].

The electrochemical behaviour of copper ions in the concentration range of 0.15 mM to 3.0 mM in 0.20 M sulphate sodium solution is shown in Fig. 5. It is noteworthy that different responses were obtained as the copper ions concentration was increased. At copper ions concentrations lower than 1.0 mM, the CVs indicated only one sharp cathodic peak at +0.070 V and one broad anodic peak at +0.400 V, with total charge passed for the anodic peak being significantly less than that for the cathodic one. This

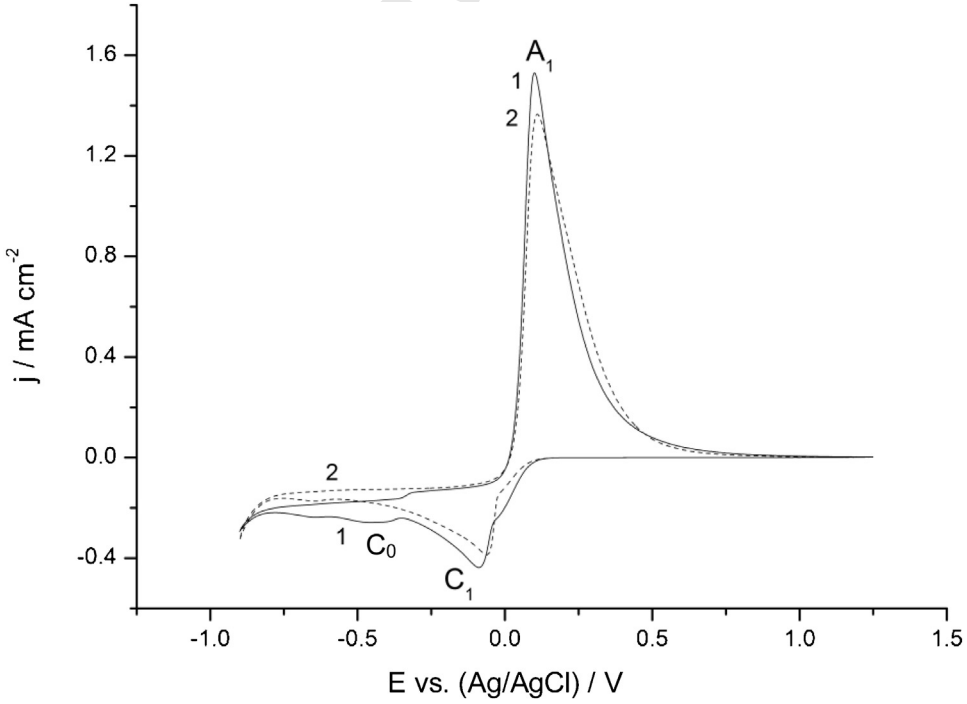

Fig. 4. Cyclic voltammograms obtained in (1) freshly as-prepared and (2) degassed oxygen-free solutions containing 3.00 mM $CuSO_4$ and 0.60 M $NaClO_4$ at 10 mV s^{-1}.

Please cite this article in press as: M. Nie, et al., Electrochemical detection of cupric ions with boron-doped diamond electrode for marine corrosion monitoring, Electrochim. Acta (2015), http://dx.doi.org/10.1016/j.electacta.2015.12.194

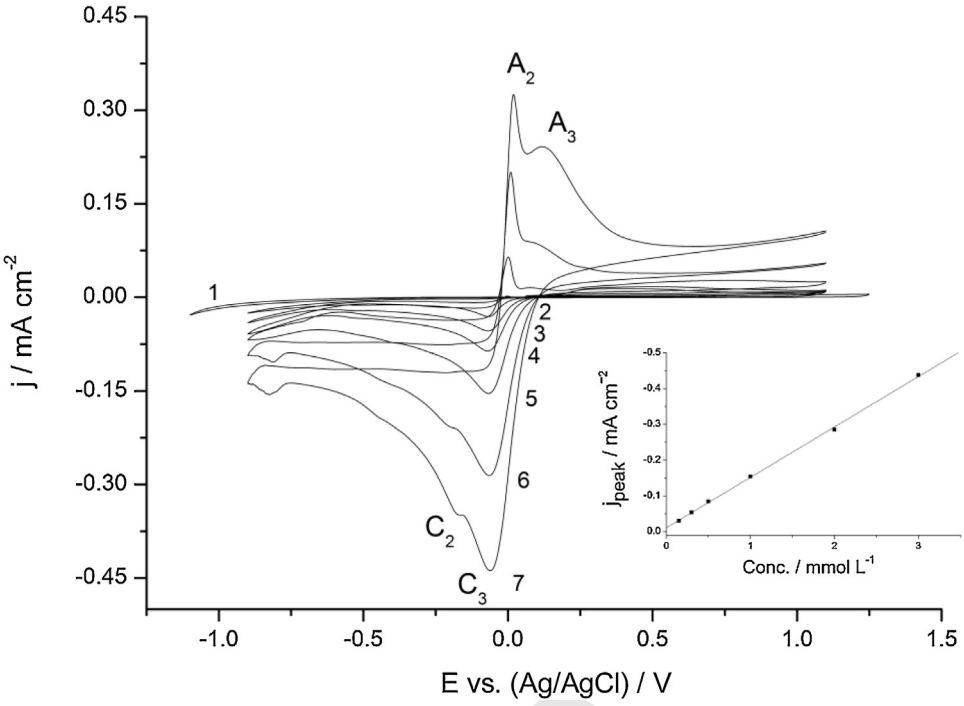

Fig. 5. Cyclic voltammograms of (1) 0, (2) 0.15, (3) 0.30, (4) 0.50, (5) 1.00, (6) 2.00 and (7) 3.00 mM $CuSO_4$ in 0.20 M Na_2SO_4 recorded at 10 mV s^{-1}. Inset shows the trend of the reduction peak current density (C_3) against the concentration of copper ions.

behaviour agrees with the previously reported electrochemical response in 0.1 M Na_2SO_4 neutral solution where the electro-deposited Cu(0) clusters on the diamond electrode surface during the cathodic process diffused away from the BDD surface into the bulk solution before being detected in the anodic scan as a result of the formation of the insulating oxide layer on the copper clusters and the electrostatic repulsion between the BDD surface and the copper clusters [14,35,36]. However, when the copper ions concentration was higher than 1.0 mM, there are two partly overlapped reduction peaks at −0.060 V and −0.175 V, and two partly overlapped oxidation peaks at +0.025 V and +0.120 V respectively. It is apparent that the peak C_3 is attributed to

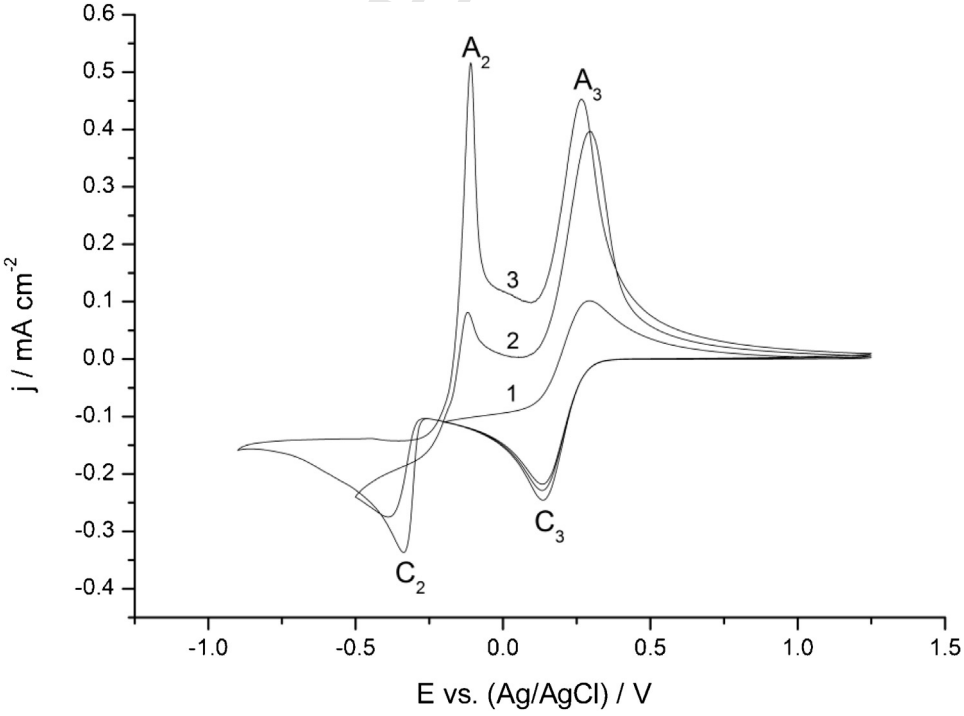

Fig. 6. Cyclic voltammograms of 3.00 mM $CuCl_2$ in 0.60 M NaCl recorded at 10 mV s^{-1} in the potential ranges (1) +1.25 V to −0.25 V, (2) +1.25 V to −0.5 V and (3) +1.25 V to −0.9 V.

Please cite this article in press as: M. Nie, et al., Electrochemical detection of cupric ions with boron-doped diamond electrode for marine corrosion monitoring, Electrochim. Acta (2015), http://dx.doi.org/10.1016/j.electacta.2015.12.194

reduction of copper ions as its peak current density increased linearly with the increase of copper ions concentration (the inset in Fig. 5), while the sharp peak A_2 is characteristic of anodic stripping of deposited metallic films. As previously proposed [35,38,55], the couple of peaks (A_3/C_3) centred at +0.040 V was attributed to the redox couple Cu^{2+}/Cu^{+}, while the other redox system (A_2/C_2) centred at –0.080 V was assigned to the redox system Cu^{+}/Cu^{0}. The appearance of the additional peaks at higher concentration of copper ions could arise from the deposition of metallic copper on the BDD surface. It was also reported [14], the diameter and density of metallic copper deposits on the BDD electrode surface increased with the increase of copper ions concentration. At higher copper concentrations, subsequent to the anodic stripping, the chemical reaction between Cu^{2+} ions accumulating on the electrode surface and the remainder of metallic copper deposits occurs to form Cu^{+} ions, which is further oxidized to Cu^{2+} ions in the positive scan appearing as peak A_3. The metallic copper deposit also acts catalyst for disproportionation of Cu^{+} ions formed by the reduction of Cu^{2+}, thus producing a relatively small peak C_2 in the negative scan.

In addition, the effect of chloride ions on separation of the metallic copper particles has been briefly examined by performing the potential cycle treatment of 1 mM $CuSO_4$ on H-, O- and F-terminated BDD electrodes from -0.6 V to +0.8 V in 0.1 M Na_2SO_4 with varying concentrations of NaCl up to 0.1 M or in 0.1 M KCl only [14]. Only one cathodic peak and one anodic peak were reported in the potential range on all three types of BDD surfaces with total charge passed for the anodic peak being considerably less than that for the cathodic one. On the contrary, experiments performed with 3.0 mM $CuCl_2$ in a 0.60 M NaCl electrolyte solution presented two well-separated pairs of peaks A_2/C_2 and A_3/C_3 for the redox couples in a potential window of –0.90 V to +1.25 V, as seen in Fig. 6. As discussed earlier [31,33,56], the cuprous ion (Cu^{+}) is not stable in aqueous media and can be easily oxidized. However, the presence of high concentrations of chloride ions stabilizes the cuprous ion by forming a highly soluble dichlorocuprous anion $CuCl_2^{-}$ through the reaction:

$$Cu^{+} + 2Cl^{-} \rightarrow CuCl_2^{-} \quad (3)$$

In an electrolyte of 0.60 M NaCl, nearly 100% of the Cu^{+} ion is complexed in the form of the $CuCl_2^{-}$ anion [33]. Considering the weak stability of the chloride-copper(II) complex, Cu^{2+} ions in 0.60 M NaCl are likely to be present as an aquo-complex rather than as the chloride-complex $CuCl^{+}$ [56]. The overall electrochemical process for copper ions in 0.60 M NaCl can be expressed as ECE procedure as below:

$$Cu^{2+} + e^{-} \rightarrow Cu^{+} \quad (4)$$

$$Cu^{+} + 2Cl^{-} \rightarrow CuCl_2^{-} \quad (3)$$

$$CuCl_2^{-} + e^{-} \rightarrow Cu^{0}_{ads} + 2Cl^{-} \quad (5)$$

The peak pair A_3/C_3 corresponds to Eq. (4) while the other peak pair A_2/C_2 corresponds to Eq. (5) in the presence of high concentration chloride ions. In light of the CV results performed at different scan rates in the potential range of –0.25 V to +1.25 V, a quasi-reversible kinetic process was observed for the reduction/oxidation of Cu^{2+}/Cu^{+} redox couple in a chloride containing media. As seen in Fig. 7, with the scan rate increased from 10 mV s^{-1} to 300 mV s^{-1}, the peak to peak potential separation for the peak pair A_3/C_3 increased from 0.180 V to 0.385 V, while the reduction peak current linearly increased with the square root of scan rate, indicating a diffusion controlled process.

Nicholson method [57] cannot be applied to calculate the apparent rate constant (k^{0}_{app}) of electron transfer process for Cu^{2+}/Cu^{+} redox couple from all the measurements performed here due to the larger peak-to-peak difference potentials obtained. Therefore, quasi-steady polarization techniques in low-field

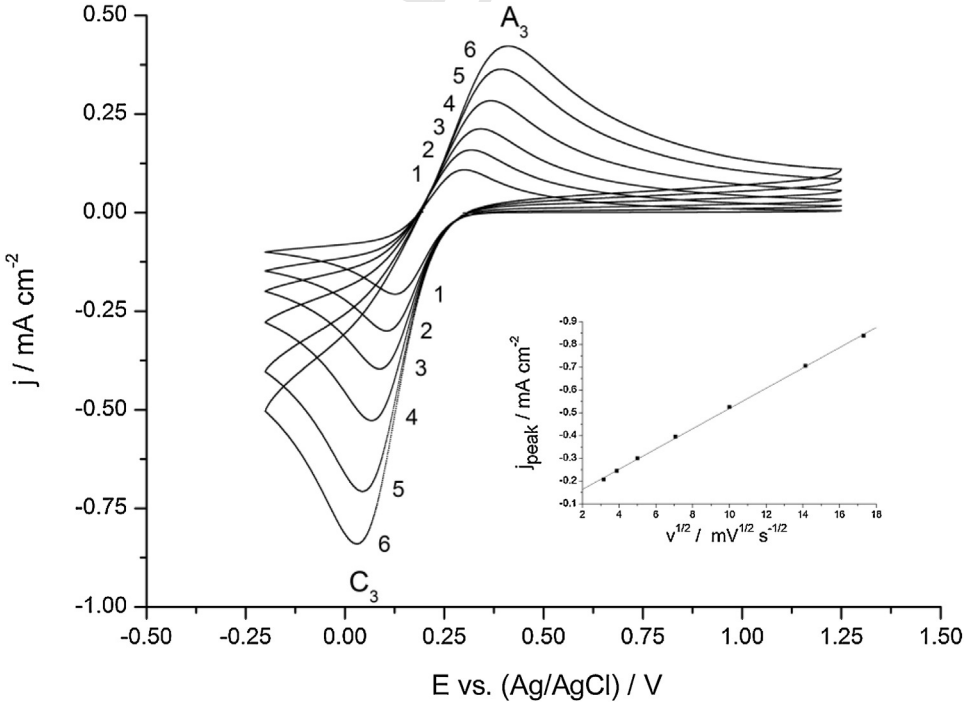

Fig. 7. Cyclic voltammograms of 3.00 mM $CuCl_2$ in 0.60 M NaCl recorded at (1) 10, (2) 25, (3) 50, (4) 100, (5) 200 and (7) 300 mV s^{-1} in the potential range of –0.25 V to +1.25 V. Inset shows the trend of the reduction peak current density *vs.* the square root of the scan rate.

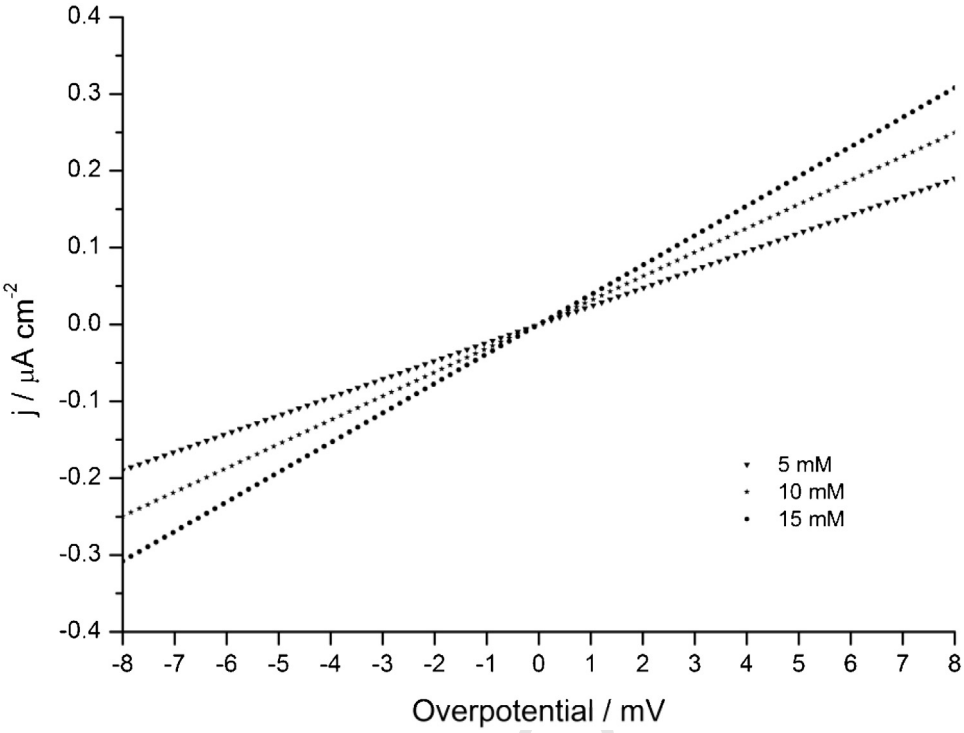

Fig. 8. Polarization curves of $CuCl_2$ at different concentrations in 0.60 M NaCl obtained under low-field conditions at 0.02 mV s^{-1}.

approximation were employed to determine k^0_{app} [44,58]. As seen in Fig. 8, under the low-field conditions, linear current response against the applied overpotential (η) was observed on the BDD electrodes for different concentrations of copper ions, and an increase of the current density is clearly evident as the concentration of Cu^{2+} ions increased from 5 to 15 mM. The Bulter-Volmer equation for the electrode response can be approximated under low-field conditions as

$$j = j_0 \frac{zF}{RT}\eta \quad (6)$$

Assuming that the transfer coefficients $\alpha_a = \alpha_c = 0.5$ and the surface concentrations of the redox couple equal to those of the

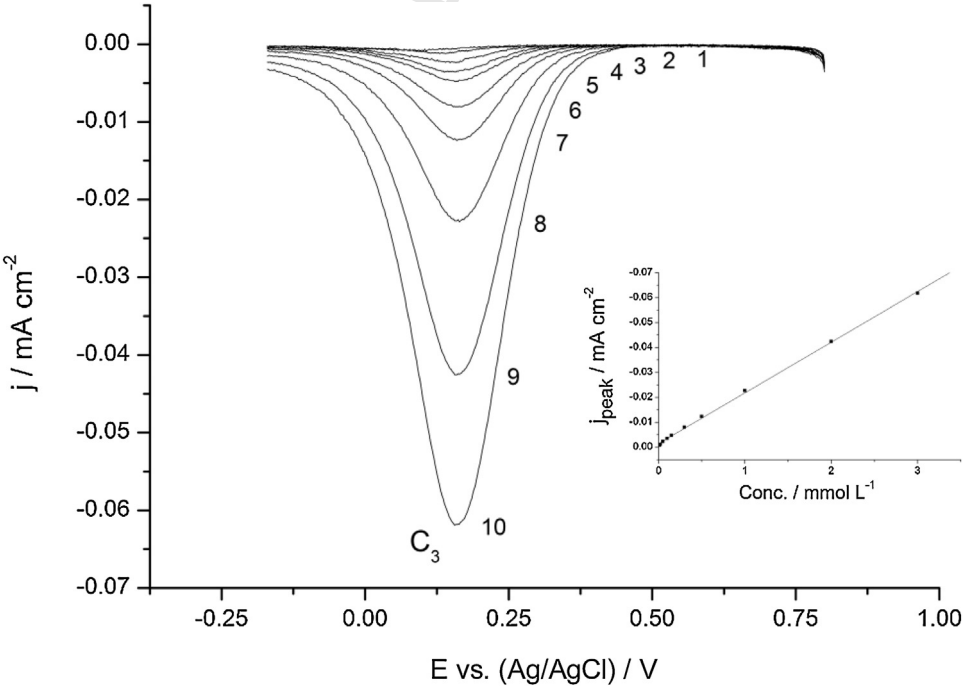

Fig. 9. DPVs of (1) 0.01, (2) 0.02, (3) 0.05, (4) 0.10, (5) 0.15, (6) 0.30, (7) 0.50, (8) 1.00, (9) 2.00 and (10) 3.00 mM $CuCl_2$ in 0.60 M NaCl. Inset shows peak current density as a function of the copper ions concentration.

Please cite this article in press as: M. Nie, et al., Electrochemical detection of cupric ions with boron-doped diamond electrode for marine corrosion monitoring, Electrochim. Acta (2015), http://dx.doi.org/10.1016/j.electacta.2015.12.194

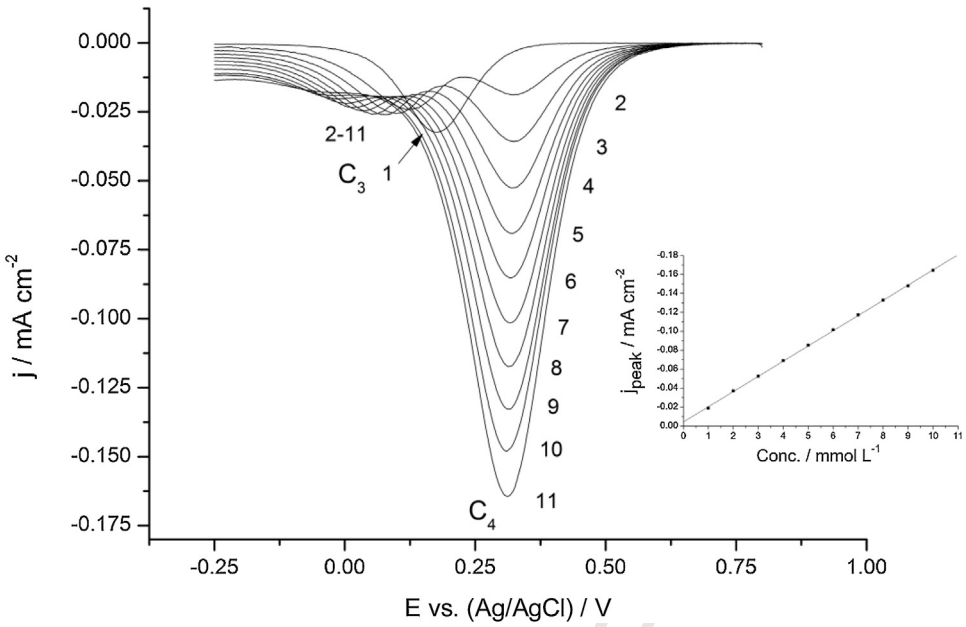

Fig. 10. DPVs of 1.0 mM $CuCl_2$ recorded with (1) 0, (2) 1.0, (3) 2.0, (4) 3.0, (5) 4.0, (6) 5.0, (7) 6.0, (8) 7.0, (9) 8.0, (10) 9.0 and (11) 10.0 mM Fe^{3+} in 0.60 M NaCl. Inset shows peak current density (C_4) as a function of the ferric ion concentration.

bulk solution (C), the exchange current density can be further approximated as

$$j_0 = Fk^0_{app}C \quad (7)$$

From the slope of plot of current density j against the applied overpotential, the exchange current density j_0 can be evaluated, thereby the apparent rate constant determined according to Eq. (7). The estimated value for the electron transfer process of the redox couple Cu^{2+}/Cu^{+} in the presence of 0.60 M Cl^- was 0.94×10^{-6} cm s^{-1}, which is in the range of $0.3\ v^{1/2} > k^0_{app} > 2 \times 10^{-5}\ v^{1/2}$ for a quasi-reversible electron-transfer process [59].

3.4. Determination of copper ions in simulated marine corrosion solution with BDD electrode using DPV technique

As DPV is known to be more sensitive than CV by removing non-faradic background currents from the current response [18,33,34,60], the determination of copper ions has been carried

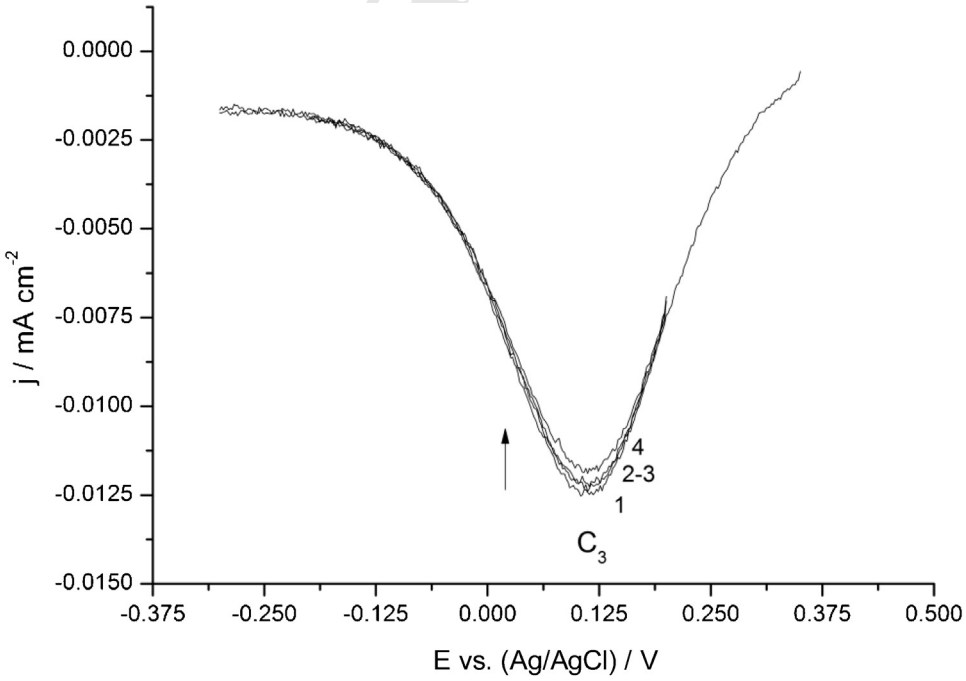

Fig. 11. DPVs obtained for 1.0 mM $CuCl_2$ with (1) 0, (2) 1.0, (3) 5.0 and (4) 10.0 mM Ni^{2+} in 0.6 M NaCl at 10 mV s^{-1}.

Please cite this article in press as: M. Nie, et al., Electrochemical detection of cupric ions with boron-doped diamond electrode for marine corrosion monitoring, Electrochim. Acta (2015), http://dx.doi.org/10.1016/j.electacta.2015.12.194

out in sodium chloride solution at the concentration of 0.60 M using the DPV technique in the presence of different concentrations of fresh aliquots of Fe^{3+}, Al^{3+} and Ni^{2+} ions.

3.4.1. Calibration plot

As shown in Fig. 9, the reduction peak currents for the Cu^{2+}/Cu^{+} process clearly increase as the concentration of copper ions increase. An excellent linear relationship with $R^2 = 0.993$ was observed between the peak current densities and the concentrations of copper ions for the cathodic peak in the concentration range of 1.0×10^{-5} M to 0.10 M. The limit of detection for copper ions was also estimated as 1.0×10^{-5} M with the established DPV technique, based on a peak current measurement for copper ions at a value 3-times greater than the background current.

3.4.2. Interferences

As previously reported [30–32], Fe^{3+}, Al^{3+} and Ni^{2+} ions are often produced with much lower concentration than that of copper ions within crevice corrosion solutions of copper alloys in marine environments and these metal ions are sometimes electrochemically active which may interfere with the detection of copper ions. The interference from ferric ions on copper detection was observed when ferric ion was added into the solution, as shown in Fig. 10. Upon the addition of equi-molar concentration of ferric ions into the solution, the peak (C_3) current for copper ions decreased by 20 % compared with the peak current without ferric ions. However, further additions of ferric ions into the solution caused no more decreases in the copper ions response up to 10-fold molar excess of ferric ions; at this concentration the peak C_4 for reduction of ferric ions on the BDD electrodes overwhelmed the copper ions response. Moreover, as seen in Fig. 10, the peak potential of copper ions shifted negatively as the iron concentration increased. The inset of Fig. 10 also shows that an excellent linear relationship exists between ferric ion concentration and peak current density with $R^2 = 0.9997$. A detailed investigation for simultaneous detection of copper and iron ions using BDD electrodes is currently on-going. The interference of aluminium ions on copper detection was also investigated on the BDD electrode and no significant interference was observed to the electrochemical response of 1.0 mM copper ions with an excess of aluminium ions in the range of 1–10 mM.

Quantification of copper in the presence of nickel ions as an interfering metal ion is shown in Fig. 11. Only a small decrease of 8% in the peak current of 1.0 mM copper ions was observed even in the presence of a 10-fold excess of nickel ions. It was also observed that better copper quantification with further reduced interference from nickel ions could be achieved when the DPV scanning was started from a lower potential of +0.20 V (traces 2–4, Fig. 11) rather than higher potential of + 0.80 V (trace 1 in Fig. 11). The reason behind this could be explained in terms of adsorptive phenomenon of nickel ions present in the solution when the electrode was imposed with a high anodic potential. In fact, adsorption phenomenon and possible further incipient oxidation of Ni^{2+} to Ni^{3+}, can occur when the potential applied to the electrode approaches +1.0 V [61].

4. Conclusions

The electrochemical response of copper ions in 0.60 M sodium perchlorate, 0.20 M sodium perchlorate and 0.60 M sodium chloride were investigated using an oxygen-terminated BDD electrode. The results highlighted a two-electron transfer process for the copper ions in perchlorate media as well as a two single-electron transfer procedure in neutral sulphate solution when the concentration of copper ions was above 1.0 mM. In high level chloride ion containing solutions, the reduction and oxidation of copper ions on the BDD electrode proceed via ECE reaction mechanism with two single-electron transfer steps and cuprous ion complexation with chloride ions. The well-separated CV peaks observed in 0.60 M NaCl solution for copper ions could ascribe to the stabilization of Cu^{+} ions in the presence of high level chloride ions by formation of $CuCl_2^{-}$ complex. The quasi-steady polarization curve measurements indicated that the electron transfer of the redox couple Cu^{2+}/Cu^{+} on the oxygen-terminated BDD surface undergoes a quasi-reversible process in chloride media with an estimated apparent constant rate of 0.94×10^{-6} cm s^{-1}.

The quantification of copper ions using DPV technique was investigated in simulated crevice corrosion microenvironments for copper alloys in marine environment and an excellent linear relationship between peak current density and copper ion concentration was achieved in the range of 1.0×10^{-5} M to 1.0×10^{-1} M, which is fairly beyond the reported concentration range of 1.0×10^{-4} M to 7.0×10^{-2} M (or 5 ppm to 5000 ppm) produced within the crevice microenvironment of copper alloys [30–32]. The presence of nickel and aluminium ions does not considerably affect the reliability of the determination of copper ions, even at greater excess of both metal ions. For ferric ions, the initial presence of ferric ions can significantly affect peak currents and potentials of copper ions on the BDD electrodes, but no additional effects are observed when the ferric ion concentration is further increased up to 10-fold excess. The inference of iron on copper ion detection could be overcome by the simultaneous detection of copper and ferric ions. More reliable quantification of copper ions in the presence of nickel was also observed by scanning from an anodic potential of +0.20 V instead of +0.80 V. The established method here is promising for corrosion monitoring of copper alloys in marine environments and further investigations are on-going.

Acknowledgements

The authors would like to thank the Engineering and Physical Sciences Research Council UK (EPSRC) and Defence Science and Technology Laboratory (Dstl) for their financial support under grant number EP/F004362/1. We also like to thank Kevin Oliver of Diamond Detectors Ltd for supplying the boron-doped diamond electrode used in this work.

References

[1] M. Pumera, A. Merkoci, S. Alegret, New materials for electrochemical sensing VII. Microfluidic chip platforms, Trends Anal. Chem. 25 (2006) 219.
[2] G. Herzog, W. Moujahid, K. Twomey, C. Lyons, V.I. Ogurtsov, On-chip electrochemical microsystems for measurements of copper and conductivity in artificial seawater, Talanta 116 (2013) 26.
[3] C. Hébert, J. Wamking, A. Depaulis, L.A. Garcon, M. Mermoux, D. Eon, P. Mailley, F. Omnès, Microfabrication, characterization and in vivo MRI compatibility of diamond microelectrodes array for neural interfacing, Mater. Sci. Eng. C 46 (2015) 25.
[4] J.H.T. Luong, K.B. Male, J.D. Glennon, Boron-doped diamond electrode: synthesis, characterization, functionalization and analytical applications, Analyst 134 (2009) 1965.
[5] O.E. Tall, N. Jaffrezic-Renault, M. Sigaud, O. Vittori, Anodic stripping voltammetry of heavy metals at nanocrystalline boron-doped diamond electrode, Electroanalysis 19 (2007) 1152.
[6] R.G. Compton, J.S. Foord, F. Marken, Electroanalysis at diamond-like and doped-diamond electrodes, Electroanalysis 15 (2003) 1349.
[7] Y. Zhou, J. Zhi, The application of boron-doped diamond electrodes in amperometric biosensors, Talanta 79 (2009) 1189.
[8] A. Kapałka, G. Foti, C. Comninellis, Determination of the Tafel slope for oxygen evolution on boron-doped diamond electrodes, Electrochem. Commun. 10 (2008) 607.
[9] A. Fujishima, Y. Einaga, T. Narasinga Rao, D.A. Tryk, Diamond Electrochemistry, Elsevier, Amsterdam, 2005.
[10] H. Girard, N. Simon, D. Ballutaud, M. Herlem, A. Etcheberry, Effect of anodic and cathodic treatments on the charge transfer of boron doped diamond electrodes, Diamond Relat. Mater. 16 (2007) 316.

Please cite this article in press as: M. Nie, et al., Electrochemical detection of cupric ions with boron-doped diamond electrode for marine corrosion monitoring, Electrochim. Acta (2015), http://dx.doi.org/10.1016/j.electacta.2015.12.194

[11] S. Ferro, A. De Battisti, Electron transfer reactions at conductive diamond electrodes, Electrochim. Acta 47 (2002) 1641.
[12] S. Szunerits, C. Jama, Y. Coffinier, B. Marcus, D. Delabouglise, R. Boukherroub, Direct amination of hydrogen-terminated boron doped diamond, Electrochem. Commun. 8 (2006) 1185.
[13] P. Actis, A. Denoyelle, R. Boukherroub, S. Szunerits, Influence of the surface termination on the electrochemical properties of boron doped diamond (BDD) interfaces, Electrochem. Commun. 10 (2008) 402.
[14] Miyamoto, Y. Tanaka, M. Furuta, T. Kondo, A. Fujishima, K. Honda, Isolation and dispersion of reduced metal particles using the surface dipole moment of F-terminated diamond electrodes, Electrochim. Acta 54 (2009) 3285.
[15] M.R. Das, M. Wang, S. Szunerits, L. Gengembre, R. Boukherroub, Clicking ferrocene groups to boron-doped diamond electrodes, Chem. Commun. (2009) 2753.
[16] Y. Coffinier, S. Szunerits, C. Jama, R. Desmet, O. Melnyk, B. Marcus, L. Gengembre, E. Payen, D. Delabouglise, R. Boukherroub, Peptide immobilization on amine-terminated boron-doped diamond surfaces, Langmuir 23 (2007) 4494.
[17] J. Wang, J.A. Carlisle, Covalent immobilization of glucose oxidase on conducting ultrananocrystalline diamond thin films, Diamond Relat. Mater. 15 (2006) 279.
[18] A. Manivannan, M.S. Seehra, D.A. Tryk, A. Fujishima, Electrochemical detection of ionic mercury at boron-doped diamond electrodes, Anal. Lett. 35 (2002) 355.
[19] A. Goodwin, A.L. Lawrence, C.E. Banks, F. Wantz, D. Omanovic, S. Komorsky-Lovric, R.G. Compton, On-site monitoring of trace levels of free manganese in sea water via sonoelectroanalysis using a boron-doped diamond electrode, Anal. Chim. Acta 533 (2005) 141.
[20] C.E. Banks, J. Kruusma, R.R. Moore, P. Tomcik, J. Peters, J. Davis, S. Komorsky-Lovric, R.G. Compton, Manganese detection in marine sediments: anodic vs cathodic stripping voltammetry, Talanta 65 (2005) 423.
[21] Y. Song, G.M. Swain, Total inorganic arsenic detection in real water samples using anodic stripping voltammetry and a gold-coated diamond thin-film electrode, Anal. Chim. Acta 593 (2007) 7.
[22] A.J. Saterlay, C. Agra-Gutiérrez, M.P. Taylor, F. Marken, R.G. Compton, Sono-cathodic voltammetry of lead at a polished boron-doped diamond electrode: application to the determination of lead in river sediment, Electroanalysis 11 (1999) 1083.
[23] G.H. Koch, M.P.H. Brongers, N.H. Thompson, Y.P. Virmani, J.H. Payer, Corrosion Cost and Preventive Strategies in the United States, FHWA-RD-01-156, National Technical Information service, Springfield, VA, 2001.
[24] L. Yang, Techniques for Corrosion Monitoring, Woodhead, Cambridge, 2008.
[25] A.A. Panova, P. Pantano, D.R. Walt, In situ fluorescence imaging of localized corrosion with pH-sensitive imaging fiber, Anal. Chem. 69 (1997) 1635.
[26] J.J. Jacobs, A.K. Skipor, P.A. Campbell, N.J. Hallab, R.M. Urban, H.C. Amstutz, Can metal levels be used to monitor metal-on-metal hip arthroplasties? J. Arthroplasty 19 (2004) 59.
[27] J. Izquierdo, L. Nagy, A. Varga, J.J. Santana, G. Nagy, R.M. Souto, Spatially resolved measurement of electrochemical activity and pH distributions in corrosion processes by scanning electrochemical microscopy using antimony microelectrode tips, Electrochim. Acta 56 (2011) 8846.
[28] J. Izquierdo, L. Nagy, A. Varga, I. Bitter, G. Nagy, R.M. Souto, Scaning electrochemical microscopy for the investigation of corrosion process: measurement of Zn^{2+} spatial distribution with ion selective microelectrodes, Electrochim. Acta 59 (2012) 398.
[29] J. Izquierdo, A. Kiss, J.J. Santana, L. Nagy, I. Bitter, H.S. Isaacs, G. Nagy, R.M. Souto, Development of Mg^{2+} ion-selective microelectrodes for potentiometric scanning electrochemical microscopy monitoring of galvanic corrosion processes, J. Electrochem. Soc. 160 (2013) C451.
[30] J.A. Wharton, K.R. Stokes, Analysis of nickel-aluminium bronze crevice solution chemistry using capillary electrophoresis, Electrochem. Commun. 9 (2007) 1035.
[31] J.A. Wharton, K.R. Stokes, The influence of nickel-aluminium bronze microstructure and crevice solution on the initiation of crevice corrosion, Electrochim. Acta 53 (2008) 2463.
[32] M. Nie, J.A. Wharton, A. Cranny, N.R. Harris, R.J.K. Wood, K.R. Stokes, Characterisation of crevice and pit solution chemistries using capillary electrophoresis with contactless conductivity detector, Materials 6 (2013) 4345.
[33] A. Cranny, N.R. Harris, M. Nie, J.A. Wharton, R.J.K. Wood, K.R. Stokes, Sensors for corrosion detection: measurement of copper ions in 3.5% sodium chloride using screen-printed platinum electrodes, IEEE Sensors J. 12 (2012) 2091.
[34] S. Neodo, M. Nie, J.A. Wharton, K.R. Stokes, Nickel-ion detection on a boron-doped diamond electrode in acidic media, Electrochim. Acta 88 (2013) 718.
[35] S. Nakabayashi, D.A. Tryk, A. Fujishima, N. Ohta, Electrochemical reduction of Cu^{2+} without surface trapping on synthetic conductive diamond electrodes, Chem. Phys. Lett. 300 (1999) 409.
[36] Y. Yamaguchi, Y. Yamanaka, M. Miyamoto, A. Fujishima, K. Honda, Hybrid electrochemical treatment for persistent metal complex at conductive diamond electrodes and clarification of its reaction route, J. Electrochem. Soc. 153 (2006) J123.
[37] J. Zak, M. Kolodziej-Sadlok, AFM imaging of copper stripping/deposition processes in selected electrolytes on boron-doped diamond thin-film electrodes, Electrochim. Acta 45 (2000) 2803.
[38] S. Tamilmani, W.H. Huang, S. Raghavan, J. Farrell, Electrochemical treatment of simulated copper CMP wastewater using boron doped diamond thin film electrodes-a feasibility study, IEEE Trans. Semicond. Manufact. 17 (2004) 448.
[39] C. Prado, S.J. Wilkins, F. Marken, R.G. Compton, Simultaneous electrochemical detection and determination of lead and copper at boron-doped diamond film electrodes, Electroanalysis 14 (2002) 262.
[40] P. Sonthalia, E. McGaw, Y. Show, G.M. Swain, Metal ion analysis in contaminated water samples using anodic stripping voltammetry and a nanocrystalline diamond thin-film electrode, Anal. Chim. Acta 522 (2004) 35.
[41] J.H. Yoon, J.E. Yang, J.P. Kim, J.S. Bae, Y.B. Shim, M.S. Won, Simultaneous detection of Cd(II), Pb(II), Cu(II), and Hg(II) ions in dye waste water using a boron doped diamond electrode with DPASV, Bull. Korea. Chem. Soc. 31 (2010) 140.
[42] G. Beamson, D. Briggs, High resolution XPS of organic polymers—the scienta database, Wiley, Chichester, 1992.
[43] S. Ferro, M. Dal Colle, A. De Battisti, Chemical surface characterization of electrochemically and thermally oxidized boron-doped diamond film electrodes, Carbon 43 (2005) 1191.
[44] A.J. Bard, L.R. Faulkner, Electrochemical methods Fundamental and Applications, Wiley, Weinheim, 2000.
[45] CRC Handbook of Chemistry and Physics, in: D.R. Lide (Ed.), 89th ed., CRC Press, 2008, 2015.
[46] S. Trasatti, O.A. Petrii, Real surface area measurements in electrochemistry, Pure & Appl. Chem. 63 (1991) 711.
[47] Y. Yano, D.A. Tryk, K. Hashimoto, A. Fujishima, Electrochemical behaviour of highly conductive boron-doped diamond electrodes for oxygen reduction in alkaline solution, J. Electrochem. Soc. 145 (1998) 1870.
[48] Y. Yano, E. Popa, D.A. Tryk, K. Hashimoto, A. Fujishima, Electrochemical behaviour of highly conductive boron-doped diamond electrodes for oxygen reduction in acid solution, J. Electrochem. Soc. 146 (1999) 1081.
[49] J.A. Bennett, J. Wang, Y. Show, G.M. Swain, Effect of sp^2-bonded nondiamond carbon impurity on the response of boron-doped polycrystalline diamond thin-film electrodes, J. Electrochem. Soc. 151 (2004) E306.
[50] M.H.P. Santana, L.A. De Faria, J.F.C. Boodts, Electrochemical characterisation and oxygen evolution at a heavily boron doped diamond electrode, Electrochim. Acta 50 (2005) 2017.
[51] L.A. Hutton, J.G. Iacobini, E. Bitziou, R.B. Channon, M.E. Newton, J.V. Macpherson, Examination of the factors affecting the electrochemical performance of oxygen-terminated polycrystalline boron-doped diamond electrodes, Anal. Chem. 85 (2013) 7230.
[52] M.B. Vukmirovic, N. Vasiljevic, N. Dimitrov, K. Sieradzki, Diffusion-limited current density of oxygen reduction on copper, J. Electrochem. Soc. 150 (2003) B10.
[53] T. Abe, G.M. Swain, K. Sashikata, K. Itaya, Effect of underpotential deposition (UPD) of copper on oxygen reduction at Pt(111) surfaces, J. Electroanal. Chem. 382 (1995) 73.
[54] T. Jiang, G.M. Brisard, Determination of the kinetic parameters of oxygen reduction on copper using a rotating ring single crystal disk assembly ($RRD_{Cu(hkl)}E$), Electrochim. Acta 52 (2007) 4487.
[55] D. Grujicic, B. Pesic, Reaction and nucleation mechanisms of copper electrodeposition from ammoniacal solutions on vitreous carbon, Electrochim. Acta 50 (2005) 4426.
[56] M. Wang, Y. Zhang, M. Muhammed, Critical evaluation of thermodynamics of complex formation of metal ions in aqueous solutions III. The system Cu(I,II)-Cl^- at 298.15 K, Hydrometall. 45 (1997) 53.
[57] R.S. Nicholson, Theory and application of cyclic voltammetry for measurement of electrode reaction kinetics, Anal. Chem. 37 (1965) 1351.
[58] J. Bockris, A.K.N. Reddy, Modern electrochemistry: an introduction to an interdisciplinary area, Plenum, New York (1973) p886.
[59] C.G. Zoski, Handbook of electrochemistry, Elsevier, Amsterdam, 2006 p. 641.
[60] W.F. Sokol, D.H. Evans, Suppression of background current in differential pulse voltammetry with solid electrodes, Anal. Chem. 53 (1981) 578.
[61] Y. Zhang, S. Yoshihara, Cathodic stripping voltammetry of nickel on boron-doped diamond, J. Electroanal. Chem. 573 (2004) 327.

Please cite this article in press as: M. Nie, et al., Electrochemical detection of cupric ions with boron-doped diamond electrode for marine corrosion monitoring, Electrochim. Acta (2015), http://dx.doi.org/10.1016/j.electacta.2015.12.194